The Euler-Lagrange Equation for Interpolating Sequence of Landmark Datasets: Applications to Cardiac Anatomy

Mirza Faisal Beg[†], Patrick Helm[‡], Michael Miller[⋆], Alain Trouvé[∗], Raimond Winslow[‡] and Laurent Younes[⋆]

Quantification of Cardiac Anatomy

Fiber organization and tissue geometry of the cardiac ventricles play a critical role in electrical propagation and force production. Global as well as local changes in ventricular geometry and fiber organization are a feature of several cardiac pathologies. Tissue geometric factors such as wall thickness are known to change in response to asynchronous electrical activation of the ventricles and fiber orientation pattern is known to adapt to changes in geometry of the heart. We are applying the tools from the emerging field of Computational Anatomy [1] to study the shape and form of the heart, in normal and diseased states. Shown below are the geometry of four dog hearts, with the two failing hearts resulting from induced cardiac hypertrophy.

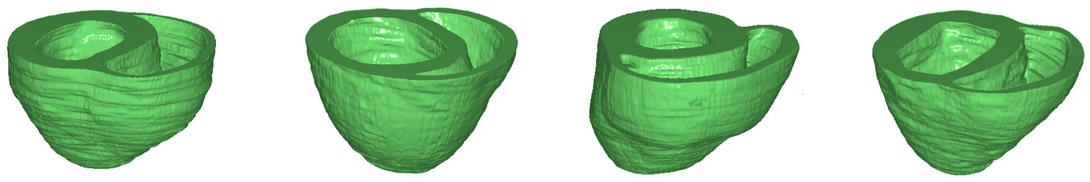

Normal(Template T_0) Normal(Target T_1) Failing(Target T_2) Failing(Target T_3)

Notice that there are marked variations in the shape and size of these hearts. Our approach to studying these shape variations involves computing dense diffeomorphic transformations for placing the disparate coordinate systems of the observed target heart anatomies into those of a chosen template. These transformations, computed from the transport equations of fluid flows, are smooth and invertible transformations thereby providing consistent mapping of the 1,2 and 3-dimensional sub-manifolds of the observed anatomy. The computation of the dense diffeomorphic transformation is achieved in two steps subsequent to rigid registration to a chosen template. First, a sparse set of landmarks are identified in each image and used to compute an initial estimate of the dense diffeomorphic transformation. This initial transformation is refined using dense image-intensity based information providing the matching forces.

The Euler-Lagrange Equation for Landmark Matching

In this work, we extend the computation of dense, non-rigid, sparse landmark-based transformations [2–4] to incorporate a time-series of landmarks. Let Ω be an open, bounded subset of $\mathbb{R}^n$ and consider an N-tuple, $\mathrm{x} = \{x_k, k = 1, \ldots, N\}$ of template landmarks in Ω. Let the corresponding N-tuple of target landmarks be a sequence in time $\mathrm{y(t)} = (y_k(t), k = 1, \ldots, N)$. Let $\phi_t : \Omega \rightarrow \Omega,\ t \in [0, 1]$ be a family of diffeomorphisms such that position of the template landmarks following the mapping $x_k(t) = \phi_t(x_k)$ are matched with the corresponding target landmarks $y_k(t)$. As candidates, we consider only the family of diffeomorphisms, G, that are isotopic to the identity via solutions to the ODE

$$\frac{\partial \phi_t}{\partial t} = v_t \circ \phi_t, \quad t \in [0, 1], \tag{1}$$

where for each $t \in [0, 1]$, $v_t \in V$, and V is a reproducing kernel Hilbert space of smooth, compactly supported velocity vector fields on Ω. Let the notation $\phi_{s,t} : \Omega \rightarrow \Omega$ denote the composition $\phi_{s,t} = \phi_t \circ (\phi_s)^{-1}$. The optimal time varying velocity field $v \in L^1([0, 1], V)$ minimizing the following energy functional

$$E(v) = \int_0^1 \|v_t\|_V^2 \mathrm{d}t + \frac{1}{\sigma^2} \sum_{k=1}^{N} \|\phi_t(x_k) - y_k(t)\|_{\mathbb{R}^n}^2$$

generates via integration from equation 1 the optimal diffeomorphic path interpolating the given landmark sequence. The Euler-Lagrange equation characterizing the extremals of the energy is found to be

$$(\nabla_v E)_t = 2v_t - \frac{2}{\sigma^2} \sum_{k=1}^{N} K_{x_k(t)}^{\left(\int_t^1 D\phi_{t,u}(x_k(t))^t (y_k(u) - x_k(u)) \mathrm{d}u\right)} = 0$$

where the term $K_x^\alpha \in V$ is the matrix reproducing kernel of V having the property $\langle K_x^\alpha, v \rangle_V = \langle v(x), \alpha \rangle_{\mathbb{R}^n}$. For target landmarks available at only one time instant $\mathrm{y} = \{y_k, k = 1, \ldots, N\}$, corresponding to the standard static landmark matching problem, the Euler-lagrange equation satisfied by the optimizer is

$$(\nabla_v E)_t = 2v_t - \frac{2}{\sigma^2} \sum_{k=1}^{N} K_{x_k(t)}^{\left(D\phi_{t,1}(x_k(t))^t (y_k - x_k(1))\right)} = 0.$$

We have implemented a gradient based algorithm algorithm for landmark matching using this Euler-Lagrange equation.

Results and Conclusion

We have developed three different automated landmark placement schemes to model the observed global and local cardiac pathologies. The first landmarking method is denoted as the arc-length method and defines landmarks at constant epicardial arc-length intervals. The second landmarking method, denoted as the radial method, defines landmarks on the epicardial wall where radial lines originating from the center of the left ventricle (LV) intersect. The third landmarking method, named radial-RV, places the origin of radial lines at the midpoint between the two right ventricle (RV) insertion points.

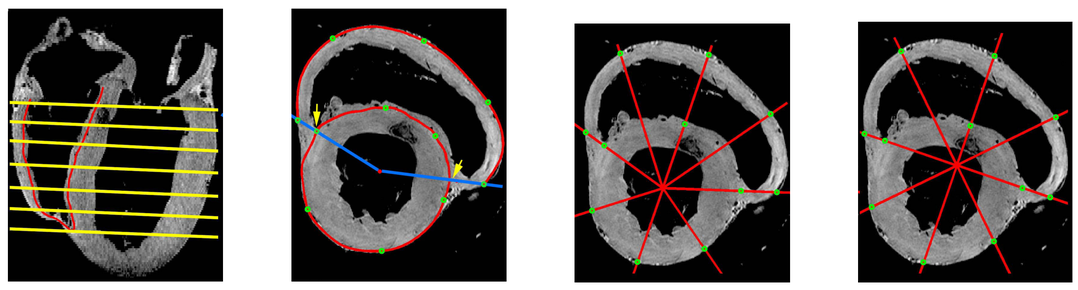

Landmarked Slices Arc-Length Radial Radial-RV

All three landmarking methods are able to accurately model pathological global tissue deformation observed in aortic or mitral valve regurgitation, chronic hypertension, or aortic stenosis. However, these landmarking methods differ significantly in accurately computing local deformations typically observed in ischemia induced heart disease. The local deformation computed via the arc-length method is inconsistent with anatomically expected deformation even when the number of landmarks is increased. Both radial landmarking methods generate anatomically consistent local tissue deformation. However, the radial-RV method has the highest accuracy in recovering both the local and global tissue deformations. Thus, radial-RV method is the preferred method for automated landmark placement.

After an initial matching is computed using landmarks, the transformation is refined with large deformation diffeomorphic image-intensity based matching [5]. The panels in the figure below show the final result of the transformation of the target anatomies to the coordinates of the template.

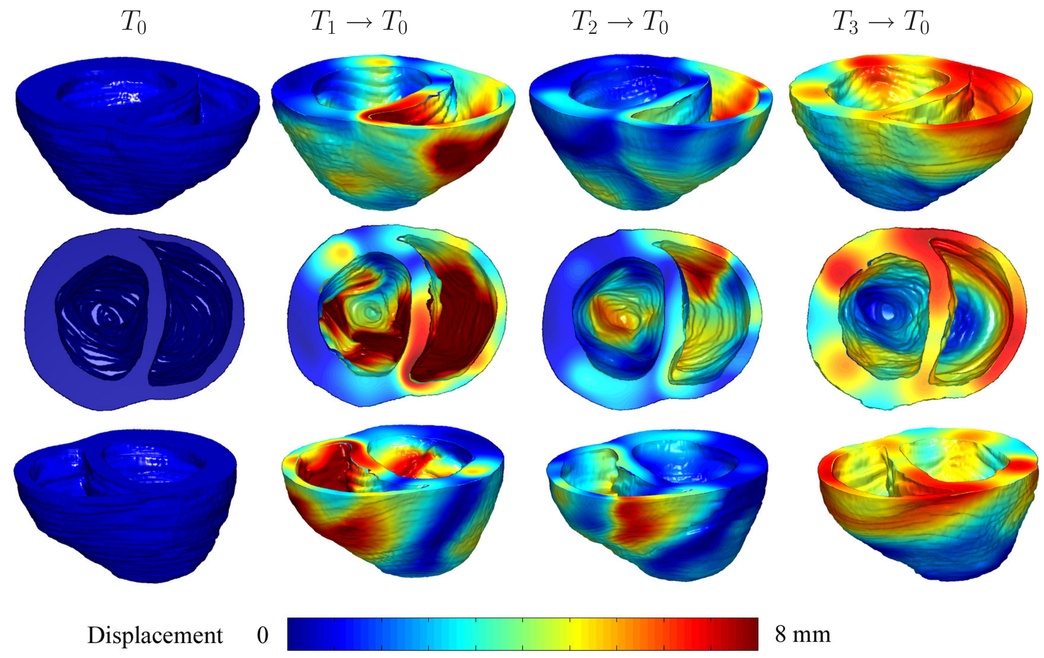

The three views above show that the target anatomies after transformation are closely registered to the template. The colormap overlaid on the surface rendering shows the magnitude of the displacement providing localized information on tissue deformation necessary for registration to template. Transforming the cardiac anatomical imagery into a common coordinate system via the dense landmark and image intensity-based diffeomorphic transformations enables us to investigate the changes in geometric features such ventricular wall thickness and allows us to compare cardiac fiber orientations in normal and diseased states.

References

[1] U. Grenander and M. I. Miller. Computational anatomy: An emerging discipline. *Quarterly of Applied Mathematics*, 56:617–694, 1998.

[2] F. L. Bookstein. Principal warps: Thin plate splines and the decomposition of deformations. *IEEE Trans. Pattern Anal. Mach. Intell.*, 11:567–585, 1989.

[3] S. Joshi and M. I. Miller. Landmark matching via large deformation diffeomorphisms. *IEEE Transactions on Image Processing*, 9(8):1357–1370, August 2000.

[4] V. Camion and L. Younes. Geodesic interpolating splines. *Lecture notes in Computer Science*, 2134:513–527, 2001.

[5] M. F. Beg, M. Miller, A. Trouvé, and L. Younes. Computing metrics via geodesics on flows of diffeomorphisms. *Accepted in the Internation Journal of Computer Vision*, 2003.

† School of Engineering Science, Simon Fraser University, 8888 University Drive, Burnaby BC V5A 1S6, Canada
∗ CMLA, École Normale Supérieure de Cachan, 61 Avenue du President Wilson, F-94235, Cachan, CEDEX, France
⋆ Center for Imaging Science and the Department of Biomedical Engineering, The Johns Hopkins University School of Medicine, Baltimore, USA
‡ Center for Cardiovascular Bioinformatics and Modeling and the Department of Biomedical Engineering, The Johns Hopkins University School of Medicine, Baltimore, USA
Center for Imaging Science http://www.cis.jhu.edu

Research supported by NIH 1 RO1 HL70894
1 P41 RR15241-01A1